IEEE Access
Multidisciplinary | Rapid Review | Open Access Journal

Received May 30, 2016, accepted June 11, 2016, date of publication June 20, 2016, date of current version August 26, 2016.

Digital Object Identifier 10.1109/ACCESS.2016.2582462

Multi-Set Space-Time Shift-Keying With Reduced Detection Complexity

IBRAHIM A. HEMADEH, (Student Member, IEEE), MOHAMMED EL-HAJJAR, (Senior Member, IEEE), SEUNGHWAN WON, (Senior Member, IEEE), AND LAJOS HANZO, (Fellow, IEEE)
University of Southampton, Southampton SO17 1BJ, U.K.

Corresponding author: L. Hanzo (lh@ecs.soton.ac.uk)

This work was supported in part by the Engineering and Physical Sciences Research Council under Projects EP/Noo4558/1 and Project EP/L018659/1, in part by the European Research Council's Advanced Fellow Grant through the Beam-Me-Up Project, and in part by the Royal Society's Wolfson Research Merit Award.

ABSTRACT In this paper, we propose a novel multi-set space-time shift keying (MS-STSK) technique, where the source bits are conveyed over two components, namely, by activating one out of M_Q dispersion matrices of STSK and M antenna combination of the N_t available antennas, in a similar fashion to spatial modulation but activating multiple antennas rather than a single antenna. This system requires a smaller number of RF chains than antenna elements (AEs) to achieve an improved throughput. We opt for STSK as the main building block of our proposed MS-STSK as a benefit of its design flexibility, where STSK is capable of providing the system with both diversity and multiplexing gains. The proposed MS-STSK system achieves both higher data rates and a lower bit error rate than the conventional STSK scheme, which is attained at the cost of increased number of AEs and a high-speed antenna switch. Furthermore, as the symbol rate of the MS-STSK system increases, its performance compared with the STSK scheme is significantly improved because of the enhanced diversity introduced by the additional AEs. Furthermore, we propose a reduced complexity detector for Quadrature Amplitude Modulation (QAM)/Phase Shift Keying (PSK) constellations, which—despite its reduced complexity—is capable of achieving the same performance as the optimal maximum likelihood detector.

INDEX TERMS MIMO, space-time shift keying, spatial modulation, *M*PSK, *M*QAM.

NOMENCLATURE

AC	Antenna Combination
AE	Antenna Element
AS	Antenna Set
ASU	Antenna Selection Unit
AWGN	Additive White Gaussian Noise
BER	Bit Error Rate
BLAST	Bell-Labs Layered Space-Time
BPC	Bits Per Codeword
CSI	Channel State Information
GSFIM	Generalised Space-Frequency Index Modulation
GSIM	Generalised Spatial Index Modulation
HL	Hard-Limiter
ICI	Inter-Channel Interference
LDC	Linear Dispersion Coding
LSSTC	Layered Steered Space-Time Coding
MBER	Minimum Bit Error Ratio
MF	Matched Filter
MIMO	Multiple-Input Multiple-Output
ML	Maximum Likelihood
MMSE	Minimum Mean Square Error
MS-STSK	Multi-Set Space-Time Shift Keying
OFDM	Orthogonal Frequency-Division Multiplexing
OSTBC	Orthogonal STBC
RAs	Receive Antennas
Rx	Receiver
ST	Space-Time
STBC	Space-Time Block Code
STSK	Space-Time Shift Keying
SM	Spatial Modulation
SNR	Signal-to-Noise Ratio
SSK	Space-Shift Keying
TA	Transmit Antenna
Tx	Transmitter

I. INTRODUCTION

Driven by the thirst for advanced wireless communications services, the demand for high-rate reliable links is significantly increased [1], [2]. For the sake of meeting this challenge, numerous solutions have been investigated, such as shifting the carrier frequencies toward higher frequency bands [3], reducing the cell sizes [4] or employing enhanced signal processing techniques [5].

Multiple-Input Multiple-Output (MIMO) techniques provide wireless communications with enhanced capacity and reliability [6]. Multiplexing techniques, such as the well-known Bell-Labs Layered Space-Time (BLAST) [7] system provide a beneficial multiplexing gain, while diversity techniques, such as the Space-Time Block Code (STBC) [8], [9], attain diversity gains at the maximum achievable normalized throughput of one. The multifunctional MIMO scheme known as Layered Steered Space-Time Coding (LSSTC) [10] combines the benefits of both the VBLAST and STBC techniques with beamforming in order to simultaneously attain a combination of these gains. Furthermore, for the sake of achieving multiplexing gains at a reduced complexity for a given spectral efficiency, Spatial Modulation (SM) was proposed in [11], where a single symbol can be transmitted over a single antenna selected from multiple antennas. SM is capable of attaining high normalized throughput at a low detection complexity with the aid of its Inter-Channel Interference (ICI) free design [12]. SM is capable of achieving a compelling performance versus complexity compromise with the aid of a single RF chain [13], [14]. Later, for the sake of attaining both multiplexing and diversity gains, the idea of SM was combined with Linear Dispersion Coding (LDC) [15], [16], resulting in the concept of Space-Time Shift Keying (STSK) [17], which subsumes both SM and Space-Shift Keying (SSK) scheme as special cases and strikes a design trade-off between the attainable multiplexing and diversity gains. Furthermore, the Generalized Spatial Modulation (GSM) concept was proposed in [18], where a specific fraction of the total number of antennas is activated in order to transmit multiple PSK/QAM symbols, while relying on implicit antenna index information. However, the GSM scheme suffers from inter-antenna interference, which may however be mitigated with the aid of sophisticated receiver techniques [19]. For the sake of further enhancing the performance of the GSM scheme, transmit precoding was applied to the transmitted symbols in [20].

Another multifunctional MIMO arrangement referred to as the STBC-SM was proposed in [21], where the low-complexity Orthogonal STBC (OSTBC) concept was combined with SM in order to provide both multiplexing and diversity gains. However, the problem imposed by OSTBC is that the maximum normalized throughput of one can be fully achieved by Alamouti's 2×2 STBC, hence in order to improve the throughput of STBC-SM, an increased number of antenna combinations should be employed, which would impose a higher complexity. Recently, Datta *et al.* [22] proposed a pair of techniques, namely Generalized Spatial Index Modulation (GSIM), which exploits the idea of SM by transmitting over multiple antennas in order to implicitly convey extra information over multiple antenna indices. The second technique proposed in [22] is referred to as Generalized Space-Frequency Index Modulation (GSFIM), which utilizes both the space and frequency indices of an Orthogonal Frequency-Division Multiplexing (OFDM) symbol to enhance the attainable throughput by conveying additional information over the combination of antennas and sub-carrier frequency indices. Furthermore, both the GSIM and GSFIM increase the attainable throughput without affecting the diversity order.

Owing to the fact that the STSK scheme is considered as a generalized version of SM, where a single dispersion matrix rather than a single antenna is activated with the aid of a modulated symbol, the existing SM detection techniques can also be employed for STSK Receivers (Rxs).

TABLE 1. List of symbols.

N_{RF}	Number of transmit RF chains
N_t	Number of transmit antennas
θ_c	Phase shift rotation
$\mathcal{O}(.)$	Complexity order
M_Q	Number of dispersion matrices, where $q = 1, \ldots, M_Q$
M_c	Constellation size, where $l = 1, \ldots, M_c$
N_c	Number of combinations, where $c = 1, \ldots, N_c$
T	Number of STSK time slots
M	Number of STSK spaces
B_{ASU}	Number of bits fed into the ASU
B_{STSK}	Number of bits fed into the STSK encoder
B	Number of MS-STSK encoded bits
$\tilde{\mathbf{X}}$	MS-STSK codeword
$\tilde{A}_{q,c}$	MS-STSK dispersion matrix
s_l	QAM/PSK symbol
$\bar{\mathbf{Y}}$	Vectorized received singal
$\bar{\mathbf{H}}$	Vectorized equivalent channel
$\mathbf{H_c}$	Activated combination effective channel
$\mathbf{h}_{c,q}$	The q-th column of the c-th effective channel $\mathbf{H_c}$
$\mathcal{X}$	Vectorized MS-STSK dispersion matrices
$\mathcal{I}$	AC activation matrix
$\mathbf{I_C}$	Identity matrix at the c-th position in $\mathcal{I}$
$\mathbf{K}$	QAM/PSK symbol activation vector
$\triangle\theta_c$	Phase-shift difference between two ACs
$\hat{\mathbf{y}}_{c,q}$	Equalized received signal by the c-th channel combination and the q-th dispersion matrix
$\hat{s}_l$	The estimate of the l-th transmitted symbol

STSK detectors can be broadly categorized as optimal [23]–[25] and suboptimal detectors [11], noting that optimality can be achieved in the context of numerous criteria, such as the ubiquitous Minimum Mean Square Error (MMSE) [26], [27], the Minimum Bit Error Ratio (MBER) [28] and the Maximum Likelihood (ML) [27] criterion etc. Suboptimal detectors having a reduced complexity typically exhibit a degraded performance.

Against this background, in this paper, we introduce the concept of Multi-Set Space-Time Shift Keying (MS-STSK), which combines the benefits of conventional SM and STSK schemes for the sake of achieving high multiplexing and diversity gains by conveying additional information over the selected Antenna Combination (AC) index, while maintaining the system's diversity gain. In our proposed MS-STSK, information bits are conveyed by both the encoded STSK codeword and the activated AC, which is defined as a combination of N_{RF} antennas out of a total of N_t Transmit Antennas (TAs), given that $N_{RF} < N_t$. This lends additional flexibility to the MS-STSK system in terms of designing the attainable multiplexing and diversity gains. Furthermore, we show that the complexity of the detector may be reduced compared to that of the Maximum Likelihood (ML) detector by employing a reduced-complexity optimal detector based on the hard-limiter (HL) ML detector concept of [29]. The novelty of this treatise can be summarized as follows:

1) We propose a novel MIMO scheme termed as the MS-STSK, which generalizes the concept of SM to a multiple antenna activation scheme, where in addition to the STSK codeword, further information bits are implicitly conveyed by the AC selection. This scheme is potentially capable of attaining both an increased transmission rate and an improved Bit Error Rate (BER) performances depending both on the specific STSK arrangement employed as well as on the number of antennas and RF chains, which affects the number of ACs.
2) The MS-STSK is a scalable scheme, which has STSK, SM and SSK as special cases. More specifically, an MS-STSK system having a single AC becomes STSK, while having a single AC and a single STSK dispersion matrix the system degenerates to SM.
3) Transmitting the same STSK codeword over different ACs would introduce a correlation between multiple MS-STSK codewords, which would inevitably reduce the performance of the system. Hence, in order to achieve the maximum attainable diversity gain, we rotate the constellation employed by a θ_c phase-shift for each AC. Imposing a phase-shift on the constellation further enhances the system's performance, since it eliminates the spatial correlation.
4) We devise a reduced-complexity optimal detector for both QAM and PSK constellations based on the hard-limiter technique [29]. The complexity order of this detector is not affected by the constellation size. Explicitly, the complexity order is improved from $\mathcal{O}(M_Q M_c N_c)$ to $\mathcal{O}(M_Q N_c)$ without degrading the optimal system performance of ML detection.
5) Finally, our simulation results demonstrate that the MS-STSK system has a better performance than the standard STSK scheme, and as the number of information bits conveyed increases, the performance improvement also increases. Furthermore, at a given normalized throughput, the MS-STSK has the same complexity order as an STSK system, whilst achieving an improved system performance.
6) The MS-STSK scheme benefits from having a flexible number of RF chains and it is capable of striking a compelling compromise between the attainable throughput as well as the BER performance. However, due to the correlation introduced by common AEs of the various ACs, the performance might degrade, which can be overcome by imposing a phase-shift on the transmitted codewords. Furthermore, the BER performance degradation may be mitigated at the cost of eroding the achievable throughput by increasing the number of transmit AEs without increasing the number of RF chains, where each AC has its own distinct transmit AEs. Finally, the achievable complexity order of the proposed MS-STSK scheme is equivalent to that of the traditional STSK scheme.

In the remainder of the paper, we present the novel concept of the MS-STSK system in Section II, while in Section III we introduce our reduced-complexity detector. In Section IV, we provide simulation results for the proposed MS-STSK system and finally, we conclude in Section V.

Notations: Bold upper case letters represent matrices; $\lfloor . \rfloor$ denotes the operation of flooring a real number to the nearest smallest following integer, while $\lfloor . \rceil$ denotes the rounding operation of a real number to the nearest integer; $mod(.)$ indicates the modulus operation; $\binom{n}{r}$ denotes the combinations without repetition of n objects taken r at a time; $(.)^T$ represents the transpose operation and $(.)^H$ represents the Hermitian transpose operation; $\mathbb{C}^{a\times b}$ indicates a matrix of complex numbers having the size $a \times b$; $\|.\|$ denotes the Frobenius norm and $|.|$ indicates the modulus of a complex number.

II. MULTI-SET SPACE-TIME SHIFT KEYING SYSTEM MODEL

In this section, we introduce the proposed MS-STSK system, which expands the idea of SM from activating a single antenna to multiple-antenna aided SM, where multiple antennas are activated in order to convey extra information. Activating multiple antennas instead of a single antenna in order to transmit an STSK codeword enhances both the system's reliability and multiplexing gain, whilst requiring a lower number of RF chains than TAs. The key system design decision is to opt for the STSK scheme for the following reasons. Firstly, the STSK scheme is capable of achieving both multiplexing and diversity gains [30], [31], whereas

other schemes, such as OSTBC's have a maximum normalized throughput of one [5], [8]. Secondly, the diversity-versus-multiplexing gain of STSK can be adjusted digitally without requiring any extra hardware. Furthermore, in contrast to GSM, by transmitting an STSK codeword rather than multiple symbols over multiple antennas, there will be no inter-symbol interference and hence no interference suppression techniques are needed. Finally, the STSK scheme constitutes a general representation of SM, hence the existing reduced complexity detectors of [23]–[25] and [32] may be appropriately adopted for our MS-STSK detector.

Again, the proposed MS-STSK system conveys information via two elements: the STSK codewords and the selected AC. It extends the conventional STSK scheme, which disperses a single PSK/QAM symbol over an activated dispersion matrix into a block-based SM-MIMO scheme, where the STSK codeword is transmitted over an appropriately selected multiple antenna combination. An AC is defined as a unique combination of the TAs out of the set of available TAs and its size is equal to the number of RF chains. The STSK scheme offers a high design flexibility, which can be translated into a trade-off between the throughput and diversity gain attained.

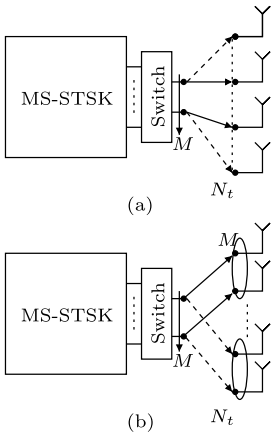

FIGURE 1. MS-STSK block diagram (a) with multiple ACs sharing one or more AEs (b) having each AC with distinct AEs.

In the proposed MS-STSK, the transmitter produces an STSK codeword to be transmitted over a specific combination of the N_t transmit antennas available using N_{RF} RF chains as shown in Figure 1-(a). The number of RF chains is equivalent to the number of spatial dimensions M over which the STSK scheme spreads the information , yielding $N_{RF} = M$ and $N_{RF} \leq N_t$. When N_{RF} is equal to the number of TAs N_t, the system becomes identical to the conventional STSK scheme. However, when N_{RF} is lower than N_t, additional information can be carried through the N_{RF} combination of TA indices without affecting the system's performance. An AC is a unique combination of $M = N_{RF}$ out of N_t TAs that can be activated using the N_{RF} RF chains employed.

A better alternative to selecting a unique AC out of the N_t available antennas would be having multiple sets of M antenna elements, as shown in Figure 1-(a), where a specific set is activated in order to transmit its index implicitly within the transmitted STSK codeword. However, this approach would limit the achievable rate due to the reduced number of ACs available, while overcoming the detrimental effects of AC correlation imposed by having some common Antenna Elements (AEs) in different ACs.

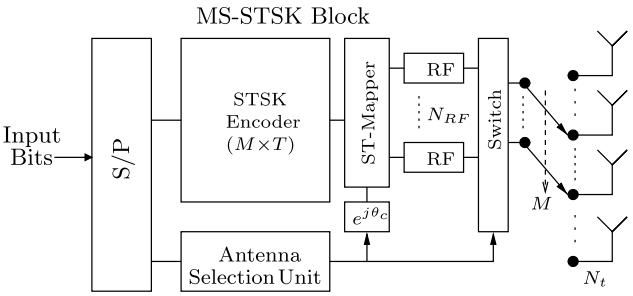

FIGURE 2. Block diagram of the proposed MS-STSK transmitter.

A. TRANSMITTER

The block diagram of the MS-STSK transmitter is shown in Figure 2. The input bit sequence is divided into two parts for the sake of encoding the MS-STSK codeword in two separate stages, namely the STSK codeword generation and the Antenna Set (AS) selection. The first $B_{STSK} = \log_2(M_c M_Q)$ bits of the input sequence are fed into the STSK encoder to produce an STSK codeword by spreading an M_c-PSK/QAM symbol over T time intervals and $M = N_{RF}$ TAs using a dispersion matrix selected from M_Q matrices.

The Antenna Selection Unit (ASU) of Figure 2 uses $B_{ASU} = \log_2(N_c)$ bits to select the specific AC over which the STSK codeword will be spread and transmitted. Given that $N_{RF} = M$ RF chains are available at the Transmitter (Tx), only an identical number of TAs can be activated simultaneously, where the combination of any M TAs is considered as a single AC. The total number of combinations is defined as $N_c = 2^k$, where k is given by

$$k = \left\lfloor \log_2 \binom{N_t}{N_{RF}} \right\rfloor. \quad (1)$$

Here, N_c is restricted to the form of 2^k in order to represent an integer number of bits, which is represented by the floor function.

Furthermore, a phase-shift θ_c, is imposed onto each of the antenna combinations by the Space-Time (ST) mapper of Figure 2 in order to reduce the correlation between the codewords associated with the same STSK coded information but different ACs for the sake of achieving the maximum attainable diversity gain, as detailed in Section II-C. The phase-shift applied to the PSK/QAM symbol rotates the whole MS-STSK codeword and it is assumed to be known for both the transmitter and receiver.

The STSK encoder, denoted here as STSK(M, N, T, M_Q, M_c), is shown in Figure 3. It outputs the space-time block defined by $\mathbf{X} = A_q s_l = [\mathbf{x_1} \dots \mathbf{x_m} \dots \mathbf{x_M}]^T$, where $\mathbf{x_m} \in \mathbb{C}^{1\times T}$ is the m-th row of $\mathbf{X}$, $s_l \in C_{M_c}$ is the M_c-PSK/QAM constellation point and $A_q \in \mathbb{C}^{M\times T}$ is the dispersion matrix selected from the set $\{A_q\}_{q=1}^{M_Q}$ satisfying the power constraint of $tr\left(A_q^H A_q\right) = T$ for $q = 1, \dots, M_Q$.

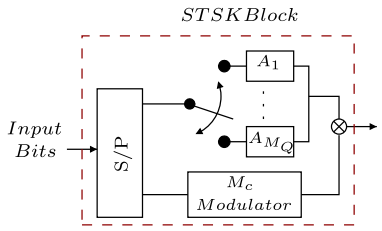

FIGURE 3. Block diagram of the STSK(M, N, T, M_Q, M_c) encoder.

Then, the ASU of Figure 2 selects the c-th AC and feeds the ST mapper with the combination's corresponding phase-shift, hence the output of the transmitter can be expressed as

$$\tilde{\mathbf{X}} = \tilde{A}_{q,c} s_l, \tag{2}$$

where $\tilde{A}_q \in \mathbb{C}^{N_t\times T}$ is the final MS-STSK dispersion matrix, which is denoted by

$$\tilde{A}_{q,c} = \begin{bmatrix} \mathbf{0} \\ \vdots \\ A_{q,m} \\ \vdots \\ \mathbf{0} \end{bmatrix} . e^{j\theta_c}, \tag{3}$$

where $A_{q,m} \in \mathbb{C}^{1\times T}$ is the m-th row of A_q, $m = 1, \dots, M$ and $\mathbf{0}$ is a vector of zeros. The phase-shift θ_c is introduced by the ASU for the sake of reducing the correlation between similar STSK codewords transmitted over one or some common TAs. The zero-valued rows of $\tilde{A}_{q,c}$ represent the inactive transmit antennas, while the complex-valued rows of $\tilde{A}_{q,c}$ indicate the activated TAs. In (3), the transmitted STSK codewords given by $\mathbf{X} \in \mathbb{C}^{M\times T}$ are converted to MS-STSK codewords represented by $\tilde{\mathbf{X}} \in \mathbb{C}^{N_t\times T}$ in order to represent the inactive TAs in the MS-STSK codeword. The system is denoted here as MS-STSK(N_t, M, N, T, M_Q, M_c).

$\mathbf{X} \in \mathbb{C}^{M\times T}$ are still of size $(M \times T)$, however the MS-STSK codeword in (3) has a size of $(N_t \times T)$ in order to represent the inactive TAs in the codeword. The system is denoted here as MS-STSK(N_t, M, N, T, M_Q, M_c).

Without loss of generality, we present two MS-STSK examples in order to further clarify the encoding process. In the first example, we consider an MS-STSK(4, 2, 2, 2, 4, 4) system having $N_t = 4$ TAs, $N_{RF} = 2$ RF chains and an STSK(2, 2, 2, 4, 4) encoder using QPSK modulation. The STSK encoder is able to generate $2^{(M_Q \times M_c)} = 2^{(4\times 4)} = 16$ distinct codewords to convey the first 4 bits of the input bit sequence. The ASU uses the next $k = \left\lfloor \log_2 \binom{N_t}{N_{RF}} \right\rfloor = \left\lfloor \log_2 \binom{4}{2} \right\rfloor = \lfloor \log_2(6) \rfloor = 2$ bits to map the STSK codewords to $2^2 = 4$ ACs. Hence, each STSK codeword $\mathbf{X} = \begin{bmatrix} \mathbf{x_1} \\ \mathbf{x_2} \end{bmatrix}$ representing B_{STSK} bits has 4 possible combinations and the MS-STSK codeword can be represented as

$$\tilde{\mathbf{X}} = \begin{bmatrix} \mathbf{x_1} \\ \mathbf{x_2} \\ \mathbf{0} \\ \mathbf{0} \end{bmatrix} e^{j\theta_1}, \quad \begin{bmatrix} \mathbf{x_1} \\ \mathbf{0} \\ \mathbf{x_2} \\ \mathbf{0} \end{bmatrix} e^{j\theta_2}, \quad \begin{bmatrix} \mathbf{x_1} \\ \mathbf{0} \\ \mathbf{0} \\ \mathbf{x_2} \end{bmatrix} e^{j\theta_3} \tag{4}$$

$$or \quad \begin{bmatrix} \mathbf{0} \\ \mathbf{x_1} \\ \mathbf{x_2} \\ \mathbf{0} \end{bmatrix} e^{j\theta_4}. \tag{5}$$

It is shown in (4) that an extra 2 bits are conveyed by selecting one out of the 4 combinations, in addition to the B_{STSK} bits carried by the STSK codeword $\mathbf{X}$.

In the second example, consider an MS-STSK(5, 2, 2, 2, 4, 4) system associated with $N_t = 5$ transmit antennas, $N_{RF} = 2$ RF chains and STSK(2, 2, 2, 4, 4) encoder with QPSK modulation, which is the same STSK encoder as in the previous example. However, the ASU here uses $k = \left\lfloor \log_2 \binom{5}{2} \right\rfloor = \lfloor \log_2(10) \rfloor = 3$ bits to map the STSK codewords to $2^3 = 8$ ACs. Hence, each STSK codeword has 8 combinations and the MS-STSK codeword can be represented as

$$\begin{aligned} \tilde{\mathbf{X}} = & \begin{bmatrix} \mathbf{x_1} \\ \mathbf{x_2} \\ \mathbf{0} \\ \mathbf{0} \\ \mathbf{0} \end{bmatrix} e^{j\theta_1}, \quad \begin{bmatrix} \mathbf{x_1} \\ \mathbf{0} \\ \mathbf{x_2} \\ \mathbf{0} \\ \mathbf{0} \end{bmatrix} e^{j\theta_2}, \quad \begin{bmatrix} \mathbf{x_1} \\ \mathbf{0} \\ \mathbf{0} \\ \mathbf{x_2} \\ \mathbf{0} \end{bmatrix} e^{j\theta_3}, \\ & \begin{bmatrix} \mathbf{x_1} \\ \mathbf{0} \\ \mathbf{0} \\ \mathbf{0} \\ \mathbf{x_2} \end{bmatrix} e^{j\theta_4}, \quad \begin{bmatrix} \mathbf{0} \\ \mathbf{x_1} \\ \mathbf{x_2} \\ \mathbf{0} \\ \mathbf{0} \end{bmatrix} e^{j\theta_5}, \quad \begin{bmatrix} \mathbf{0} \\ \mathbf{x_1} \\ \mathbf{0} \\ \mathbf{x_2} \\ \mathbf{0} \end{bmatrix} e^{j\theta_6}, \\ & \begin{bmatrix} \mathbf{0} \\ \mathbf{x_1} \\ \mathbf{0} \\ \mathbf{0} \\ \mathbf{x_2} \end{bmatrix} e^{j\theta_7} \; or \; \begin{bmatrix} \mathbf{0} \\ \mathbf{0} \\ \mathbf{x_1} \\ \mathbf{x_2} \\ \mathbf{0} \end{bmatrix} e^{j\theta_8}. \end{aligned} \tag{6}$$

where an additional 3 bits are conveyed by selecting one of the 8 combinations of $\tilde{\mathbf{X}}$.

B. MS-STSK RECEIVER

Consider a $(N_t \times N_r)$-element MIMO system, where N_r is the number of Receive Antennas (RAs) and let $\mathbf{H} \in \mathbb{C}^{N_r\times N_t}$ denote the zero-mean and unity-power channel matrix between all the TAs and RAs and $\mathbf{V} \in \mathbb{C}^{N_r\times T}$ the zero-mean Additive White Gaussian Noise (AWGN) of power N_0. The

block-based received vector can be expressed as

$$\mathbf{Y} = \mathbf{H}\tilde{\mathbf{X}} + \mathbf{V}, \tag{7}$$

where $\mathbf{Y} \in \mathbb{C}^{N_r \times T}$ represents the received block-based signal and $\tilde{\mathbf{X}}$ is the transmitted MS-STSK codeword of (2). By applying the vectorial stacking operation to the STSK received codeword in the standard STSK system, the system model is equivalent to an SM system, hence rather than activating a single antenna, a single dispersion matrix is activated [17]. In MS-STSK, to generalize the system model we follow the same vectorized representation. After applying the vectorization operation, the received MS-STSK signal can be expressed as

$$\bar{\mathbf{Y}} = \bar{\mathbf{H}}\mathcal{X}\mathcal{I}\mathbf{K} + \bar{\mathbf{V}}, \tag{8}$$

where the equivalent vectorized matrices are given by

$$\bar{\mathbf{Y}} = vec(\mathbf{Y}) \in \mathbb{C}^{N_r T \times 1}, \tag{9}$$

$$\bar{\mathbf{H}} = \mathbf{I} \otimes \mathbf{H} \in \mathbb{C}^{N_r T \times N_t T}, \tag{10}$$

$$\bar{\mathbf{V}} = vec(\mathbf{V}) \in \mathbb{C}^{N_r T \times 1}, \tag{11}$$

$$\mathcal{X} = [vec(\tilde{A}_{1,1}) \dots vec(\tilde{A}_{q,c}) \dots vec(\tilde{A}_{q,N_c})] \in \mathbb{C}^{N_t T \times N_c M_Q}, \tag{12}$$

with $\mathbf{I}$ being a $(T \times T)$-element identity matrix and $\otimes$ is the Kronecker product used for vectorising the channel matrix. Moreover, the AC is selected by the matrix $\mathcal{I} \in \mathbb{C}^{N_c M_Q \times M_Q}$ and it is described as

$$\mathcal{I} = [\mathbf{0} \dots \underset{\substack{\downarrow \\ c-th\ element}}{\mathbf{I_C}} \dots \mathbf{0}]^T, \tag{13}$$

where $\mathbf{I_C}$ is a $(M_Q \times M_Q)$-element identity matrix, which is used for selecting the c-th combination of the MS-STSK equivalent dispersion matrix set. Furthermore, the transmitted symbol used for activating the q-th dispersion matrix $\mathbf{K} \in \mathbb{C}^{M_Q \times 1}$ is expressed as

$$\mathbf{K} = [\underbrace{0, \dots, 0}_{q-1}, s_l, \underbrace{0, \dots, 0}_{M_Q - q}]^T, \tag{14}$$

where s_l represents the M_c-PSK/QAM constellation point as shown in (2). In order to activate the q-th dispersion matrix over the c-th AC, the modulated symbol s_l is located at the q-th index of $\mathbf{K}$ and the AC activation identity matrix $\mathbf{I_C}$ at the c-th position of $\mathcal{I}$. Equation (8) can be represented as

$$\bar{\mathbf{Y}} = \begin{bmatrix} \mathbf{H} & \mathbf{0} \\ \mathbf{0} & \mathbf{H} \end{bmatrix} \begin{bmatrix} \dots & \hat{A}_{q,1} & \dots \\ \vdots & \vdots & \vdots \\ \dots & \hat{A}_{q,c} & \dots \\ \vdots & \vdots & \vdots \\ \dots & \hat{A}_{q,N_c} & \dots \end{bmatrix} \begin{bmatrix} \mathbf{0} \\ \vdots \\ \mathbf{I_C} \\ \vdots \\ \mathbf{0} \end{bmatrix} \begin{bmatrix} 0 \\ \vdots \\ s_l \\ \vdots \\ 0 \end{bmatrix} + \bar{\mathbf{V}}, \tag{15}$$

where $\hat{A}_{q,c} = vec(\tilde{A}_{q,c}) \in \mathbb{C}^{N_t T \times 1}$.

The SM-equivalent transmit signal $\mathbf{K}$ activates $M_Q M_c$ distinct MS-STSK codewords having the c-th combination, hence the receiver should be able to detect one of the $M_Q M_c N_c$ legitimate transmitted signal vectors.

Given that all antenna elements at the Tx and Rx are sufficiently far apart to experience an uncorrelated channel, the vectorized system model of (8) has zero ICI. Now, given the availability of Channel State Information (CSI) at the Rx side, an ML detector may be invoked for detecting the estimates of the dispersion matrix index, the symbol constellation index and the AC index denoted by q, l and c, respectively, which are represented by $\hat{q}$, $\hat{l}$ and $\hat{c}$. Hence, the ML detector is expressed as

$$< \hat{q}, \hat{l}, \hat{c} > = \arg\min_{q,l,c} \left\| \bar{\mathbf{Y}} - \bar{\mathbf{H}}\mathcal{X}\mathcal{I}_c\mathbf{K}_{q,l} \right\|^2, \tag{16}$$

$$= \arg\min_{q,l,c} \left\| \bar{\mathbf{Y}} - s_l \left(\bar{\mathbf{H}}_c\mathcal{X}\right)_q \right\|^2, \tag{17}$$

where $\left(\bar{\mathbf{H}}_c\mathcal{X}\right)_q$ is the column vector of $\left(\bar{\mathbf{H}}\mathcal{X}\right)_q$ after selecting the c-th AC by activating the c-th identity matrix in $\mathcal{I}$ and nulling the other $(N_c - 1)$ identity matrices, hence yielding $\mathcal{I} = \mathcal{I}_c$.

C. MULTI-SET PHASE-SHIFT

Since having common antenna elements in different ACs would impose correlation between the MS-STSK codewords, a pair techniques are invoked here to overcome this effect, namely using ACs relying on distinct AEs or by applying a phase-shift to each MS-STSK codeword. When distinct sets of M antenna elements are activated to transmit each MS-STSK codeword combination, where we have $\left(\tilde{A}_{q,c}\tilde{A}^H_{q,c'}\right) = 0$ given that $c \neq c'$, the correlation between the multiple ACs introduced by their common AEs is eliminated. Hence, no phase-shift is required to overcome its effect. However, when all AEs are allocated in all ACs, the AC correlation would severely degrade the performance of the scheme, especially when the number of shared AEs between multiple ACs is increased.

As mentioned in Section II-A, a distinct phase-shift θ_c of the c-th AC is introduced by the ASU to rotate the QAM/PSK constellation for the sake of achieving the maximum attainable diversity gain introduced by the additional sufficiently-spaced TAs, which is known at both the transmitter and receiver [33]. Dispensing with the phase-shift would only influence the diversity gain. The diversity gain of the MS-STSK system might become degraded by the correlation introduced by MS-STSK codewords having similar STSK codewords, when sharing one or more antenna elements in their set of AC. This degradation may be mitigated by rotating the transmitted codewords with the aid of simply rotating the modulated symbol.

Owing to the fact that symmetrical modulation schemes are employed, the ACs phase-shifts introduced by the ASU should not overlap the shifted symbols of other constellation points, since the overlapped constellation points produce identical of presumably different MS-STSK codewords. Figure 4 shows an M_c-QAM constellation, where after

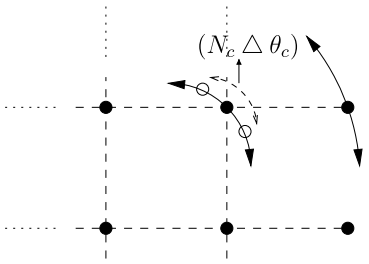

FIGURE 4. Phase-shifts of different ACs for M_c-QAM constellation.

applying N_c phase-shifts for all combinations, the resultant constellation points are spread over an angle of $N_c \triangle \theta$, where $\triangle\theta$ denotes the phase difference between two adjacent combinations, yielding $\triangle\theta = \theta_{c+1} - \theta_c$. When we have $\triangle\theta = \pi/2$, the symmetrical constellation points overlap with each other. Similarly, Figure 5 shows the angular spread of N_c phase-shifts applied to an M_c-PSK constellation. In M_c-PSK schemes, the constellation points are equally separated with an angle $\triangle\phi$ and shifting the different combinations by an angle of $\triangle\theta_c = \triangle\phi$ overlaps the different constellation points with each other, which results in having the same MS-STSK codeword for different input bit sequences.

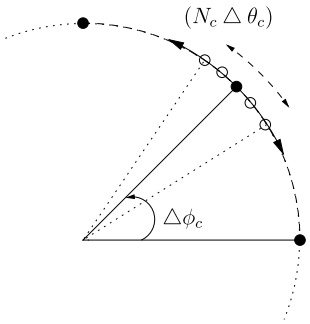

FIGURE 5. Mapping of phase-shifts of different ACs for M_c-PSK constellation.

The value of θ_c for all modulation schemes is expressed as

$$\theta_c = (-\frac{N_c}{2} + c - 1) \triangle \theta_c, \tag{18}$$

$$\triangle\theta_c \neq C\theta_b, \tag{19}$$

where C is an integer and θ_b is the angular difference between any two symbols having the same amplitude, i.e. symbols located on the same ring with different angles. Equation (18) describes the phase-shifts of all combinations around a specific QAM/PSK symbol, as shown in Figures 4 and 5. The inequality condition in (19) ensures that the combination of any STSK codewords does not overlap with any other STSK codeword. Having overlapping AC symbols would affect the performance of the detector, since the rotation of an STSK codeword $A_q\, s_l$ by an angle of $C\theta_b$ results in it overlapping with another codeword $A_q\, s_{l+1}$, when s_{l+1} has a phase of $k\theta_b$. In this case, if the detector fails to detect the activated TA correctly, then the decoder would decode $A_q\, s_{l+1}$ instead of the transmitted symbol $A_q\, s_l$.

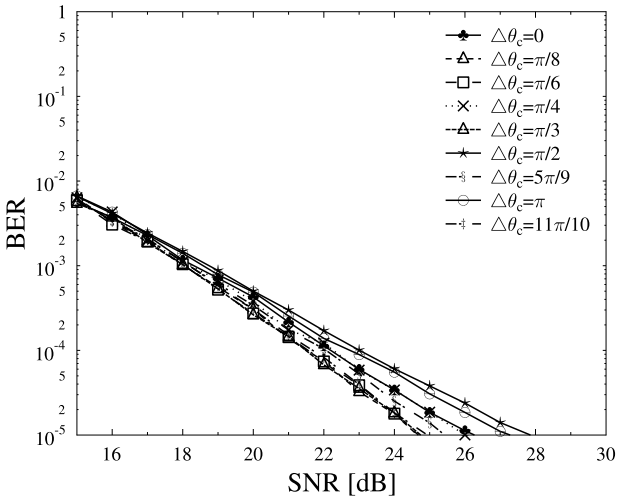

FIGURE 6. The BER performance of MS-STSK(4,2,2,2,4,16)$|_{\text{QAM}}$ with $\triangle\theta_c = 0, \pi/8, \pi/6, \pi/4, \pi/3, \pi/2, 5\pi/9, \pi$ and $11\pi/10$.

Figure 6 shows the comparison of different phase values of $\triangle\theta_c$ in conjunction with 16-QAM modulation. Consider an MS-STSK(4,2,2,2,4,16) scheme using QAM that has $N_c = 4$ ACs in conjunction with the following phase-shift values of $\triangle\theta_c = 0, \pi/8, \pi/6, \pi/4, \pi/3, \pi/2, 5\pi/9, \pi$ and $11\pi/10$. The performance of the system using $\triangle\theta_c = \pi/8, \pi/6$ and $11\pi/10$ is the highest, while the gain is the lowest for $\triangle\theta_c = \pi/2$ and π. The fact that the performance of the system associated with $\triangle\theta_c = \pi$ is slightly better than that of $\triangle\theta_c = \pi/2$ is due to the specific number of phase-shift-induced overlaps of different ACs. Explicitly, when $\triangle\theta_c = \pi$, the ACs phase-shifts happen to overlap with two constellation points, while for $\triangle\theta_c = \pi/2$ they overlap with four points, hence the BER increases for the latter. For example, consider the specific constellation points shown in Figure 4 shifted by $\triangle\theta_c = \pi/2$ over 4 combinations. The resultant symbols are shifted to the other 3 constellation points in addition to the selected symbol, which then spreads them over an activated dispersion matrix and produces codewords that are identical to another 3 MS-STSK codewords. This phenomenon can be expressed as

$$\tilde{\mathbf{X}}_1 = \begin{bmatrix} \mathbf{0} \\ \vdots \\ A_{q_1,m_1} \\ \vdots \\ \mathbf{0} \end{bmatrix} .s_{l_1}.e^{j\theta_1} = \begin{bmatrix} \mathbf{0} \\ \vdots \\ A_{q_1,m_1} \\ \vdots \\ \mathbf{0} \end{bmatrix} .s_{l_2} = \tilde{\mathbf{X}}_2. \tag{20}$$

Similarly, Figure 7 shows the comparison of different phase values of $\triangle\theta_c$ in conjunction with 8-PSK modulation. Consider an MS-STSK(4,2,2,2,2,8)$|_{\text{PSK}}$ scheme that has $N_c = 4$ ACs relying on $\triangle\theta_c = 0, \pi/8, \pi/6, 5\pi/9, 11\pi/10$ and $\pi/16$. The best performance of the system is achieved with the aid of $\triangle\theta_c = \pi/16$, while the lowest is attained at $\triangle\theta_c = 0$.

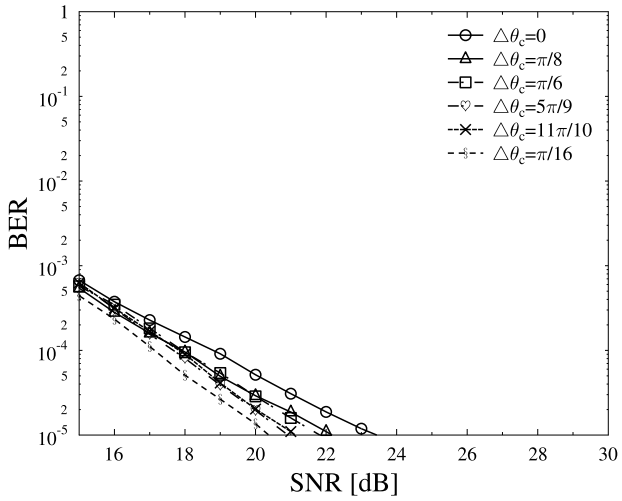

FIGURE 7. The BER performance of MS-STSK(4,2,2,2,2,8)$|_{\text{PSK}}$ with $\Delta\theta_c = 0, \pi/8, \pi/6, 5\pi/9, 11\pi/10$ and $\pi/16$.

D. MS-STSK THROUGHPUT

The main aim of the MS-STSK scheme is to improve the STSK throughput by carrying extra information over the antenna combination index, in a similar manner to the SM. The first B_{STSK} bits of the input sequence are conveyed by an STSK codeword, while the next B_{ASU} bits select the activated TAs. Hence, the total number of transmitted Bits Per Codeword (BPC) is equal to

$$B = \log_2(M_c M_Q N_c) = B_{STSK} + B_{ASU}. \text{(BPC)} \qquad (21)$$

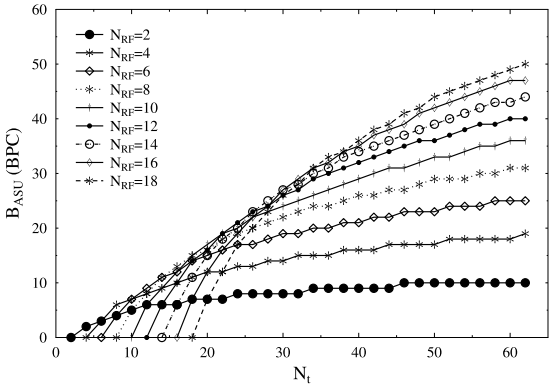

FIGURE 8. The number of extra bits per codeword (BPC) carried by the AS index versus the number of TAs N_t as a function of the number of RF chains N_{RF}.

Figure 8 illustrates the total number of bits B_{ASU} carried by the AS index versus the number of TAs N_t as a function of the number of RF chains N_{RF}. The number of TAs is bounded as $N_{RF} \leq N_t \leq 64$, where we have $N_{RF} = 2, 4, 6, 8, 10, \ldots, 32$ RF chains. It is shown in the figure that as the ratio of the number of TAs with respect to the number of RF chains available increases, the value of B_{ASU} increases. However, carefully choosing the number of AEs and RF chains at the design stage is critical for the sake of achieving an enhanced throughput with minimum requirements. When the number of RF chains is equal to that of the TAs available, the system becomes a standard STSK system and the multiplexing-versus-diversity trade-off is decided by the design of the specific STSK encoder. However, when the number of TAs exceeds the number of RF chains and we have $k \geq 1$, then the system inherits the benefits of MS-STSK.

It should also be noted from Figure 8 that the intersection between the different curves implies that the same value of B_{ASU} may be achieved with the aid of different TAs-RF chain combinations. For example, when the value of N_{RF} is either 4 or 6 at a fixed number of AEs $N_t = 10$, the value of B_{ASU} is equal to 7 BPC. Moreover, to achieve $B_{ASU} = 16$ BPC, the system may have in conjunction either $N_{RF} = 6$ with $N_t = 22$ or $N_{RF} = 16$ with $N_t = 22$.

The specific design of the STSK encoder remains pivotal for the MS-STSK system design, since the total number of RF chains should be equal to the spatial dimension of the STSK codeword given by $N_{RF} = M$. However, since the STSK encoder is digitally configured, the specific choice of the M_Q and M_c values becomes crucial, as it is in standard STSK systems.

III. REDUCED COMPLEXITY MS-STSK DETECTOR

In order to detect the activated TA combination at the receiver in addition to the STSK codeword's estimation, the optimal ML detector presented in Equations (16) and (17) imposes a complexity order of $\mathcal{O}(M_Q M_c N_c)$. Furthermore, adding multiple sets of antennas in order to convey extra information as in MS-STSK imposes a higher complexity on the detector. Accordingly, we can rely on a range of low-complexity SM detection techniques for the sake of reducing the complexity of our MS-STSK system.

Again, SM detection techniques may be divided into two main categories, namely optimal detectors [23]–[25] and suboptimal detectors [11]. The reduced complexity optimal detectors are capable of maintaining the full search based ML detector's performance. On the other hand, suboptimal detectors aim for reducing the complexity of the detector at the cost of tolerating some performance loss. Here, we are interested in achieving the optimal MS-STSK performance in order to accomplish the objective that MS-STSK was originally design for, namely, achieving an increased throughput at an enhanced performance.

Owing to the fact that our system is based on hard-decision detection, we employ a reduced complexity ML detector based on the HL aided SM detector of [25] and [29], while the complexity order of HL detectors is reduced with the aid of separating the estimation processes of each part of the received signal, namely $\hat{q}$, $\hat{l}$ and $\hat{c}$. In what follows, we propose a HL assisted detector for our MS-STSK scheme based on the reduced complexity ML detector of hard-decision based SM systems [25] for M_c-QAM constellations and on [32] for M_c-PSK constellations.

Let us assume that the the channel information is perfectly estimated at the receiver, and recall the vectorized

representation of the SM-STSK in (8). Then, in order to apply SM-aided detectors, the effective channel at the receiver of the MS-STSK scheme can be expressed as

$$\mathbf{H_c} = \bar{\mathbf{H}}\mathcal{X}\mathcal{I}_c, \tag{22}$$

where $\mathbf{H_c} = [\mathbf{h}_{c,1} \ldots \mathbf{h}_{c,M_Q}] \in \mathbb{C}^{N_r T \times M_Q}$. Each column vector of $\mathbf{H_c}$ given by $\mathbf{h}_{c,q} \in \mathbb{C}^{N_r T \times 1}$, is equivalent to an SM system having M_Q TA. The c-th activated identity matrix $\mathbf{I_C}$ in $\mathbf{H_c}$ configures the system as an SM arrangement with M TAs, since $\mathbf{I_C}$ nulls the coefficients of the inactive TAs, while maintaining the coefficients of the $M = N_{RF}$ activated TAs.

Lemma 1: The effect of the channel could be equalized by applying a vector-to-vector Hermitian transpose to each column vector of $\mathbf{H_c}$*, for the sake of estimating the modulated symbol* $< \hat{l} >$ *separately from* $< \hat{q}, \hat{c} >$*. The value of* $< \hat{l} >$ *is estimated by mapping the equalized received signal to the constellation employed, while the estimation of* $< \hat{q}, \hat{c} >$ *is determined by a full-search based vector-to-vector detection. Hence, the complexity order of the system is reduced from* $\mathcal{O}(M_Q M_c N_c)$ *to* $\mathcal{O}(M_Q N_c)$*, regardless of the QAM/PSK alphabet employed.*

According to (22), the channel $\bar{\mathbf{H}}$ is transformed to an equivalent channel $\mathbf{H_c}$ that contains all the system's dispersion matrices and ACs for the sake of applying vector-to-vector Matched Filter (MF) equalization as

$$\hat{\mathbf{y}}_{c,q} = \frac{\mathbf{h}_{c,q}^H \bar{\mathbf{Y}}}{\|\mathbf{h}_{c,q}\|^2}, \tag{23}$$

where $\hat{\mathbf{y}}_{c,q}$ is the received equalized symbol after applying MF of the q-th column of the c-th AC equivalent channel. Next, the value of $\hat{\mathbf{y}}_{c,q}$ is used to estimate the M_c-QAM/PSK symbol.

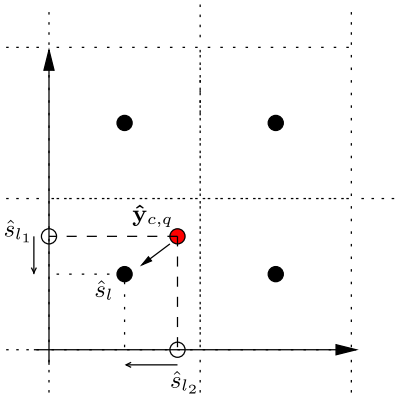

FIGURE 9. The received QAM symbol after equalization $\hat{\mathbf{y}}_{c,q}$ is viewed as a pair of PAM symbols $\hat{s}_{l_1}$ and $\hat{s}_{l_2}$, in order to determine the estimate of the transmitted symbol $\hat{s}_l$.

Two different techniques are used for detecting the M_c-QAM constellations [25] and M_c-PSK constellations [32]. Figure 9 shows the equalized symbol $\hat{\mathbf{y}}_{c,q}$ of a QAM constellation, which is used for determining the estimate $\hat{s}_l$ of the transmitted symbol, by simply dividing the QAM symbol into a pair of PAM symbols $\hat{s}_{l_1}$ and $\hat{s}_{l_2}$ for M_{c_1}-PAM and M_{c_2}-PAM constellations, respectively. Therefore, based on [25], the value of $\hat{s}_l$ can be determined as

$$\hat{s}_l = \Re(\hat{s}_l) + j\Im(\hat{s}_l), \tag{24}$$

where $\Re(\hat{s}_l)$ and $\Im(\hat{s}_l)$ are the real and imaginary parts of $\hat{s}_l$, respectively. Both the real and imaginary parts are further detailed as

$$\Re(\hat{s}_l) = \min\left\{\max\left\{D_1 - 1, -M_{c_1} + 1\right\}, M_{c_1} - 1\right\}, \tag{25}$$

and

$$\Im(\hat{s}_l) = \min\left\{\max\left\{D_2 - 1, -M_{c_2} + 1\right\}, M_{c_2} - 1\right\} \tag{26}$$

respectively, where $D_1 = 2\left\lfloor \frac{\Re(\hat{s}_l)+1}{2} \right\rceil$ and $D_2 = 2\left\lfloor \frac{\Im(\hat{s}_l)+1}{2} \right\rceil$ are determined by $\hat{s}_{l_1}$ and $\hat{s}_{l_2}$, respectively.

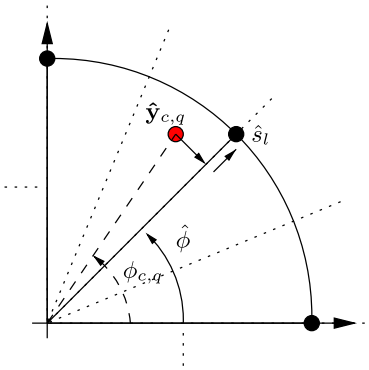

FIGURE 10. The angle $\phi_{c,q}$ of the received PSK symbol after equalization $\hat{\mathbf{y}}_{c,q}$ is carried out in order to determine the estimate of the phase of the transmitted symbol $\hat{\phi}$.

On the other hand, to determine the estimate of a PSK symbol, only the angle of the equalized symbol is required. Figure 10 shows an equalized PSK symbol $\hat{\mathbf{y}}_{c,q} = |\hat{\mathbf{y}}_{c,q}| e^{\phi_{c,q}}$, which falls within the angular decision boundary of a specific PSK constellation point. Since PSK is a constant-envelope constellation, we only need the symbol's phase angle in order to determine the estimate of the M_c-PSK transmitted symbol, hence the estimate of the transmitted M_c-PSK symbol angle can be expressed as [32]

$$\hat{\phi} = \frac{2\pi}{M_c} mod\left\{\lfloor \phi_{c,q}, M_c \rceil\right\}, \tag{27}$$

where the estimate of the transmitted symbol can be simply formulated as $\hat{s}_l = R_{M_c} e^{j\hat{\phi}}$, where R_{M_c} represents the M_c-PSK constellation radius.

After determining the estimate of s_l, the detector applies vector-by-vector full-search over all the legitimate combinations of dispersion matrices in order to determine $< \hat{q}, \hat{c} >$. Hence, the reduced-complexity ML search can be expressed as [25]

$$< \hat{q}, \hat{c} > = \arg\min_{q,c} \left(|\hat{\mathbf{y}}_{c,q} - \hat{s}_l|^2 - |\hat{\mathbf{y}}_{c,q}|^2 \right) \|\mathbf{h}_{c,q}\|^2. \tag{28}$$

To this end, it is clear that the complexity order of the ML detector can be reduced to $\mathcal{O}(M_Q N_c)$ regardless of the specific constellation size by employing the above HL-ML detector. Hence, by applying full search both for q and c over the entire search-space of M_Q and N_c, respectively, regardless of the constellation size, *Lemma 1* is guaranteed. The reduced-complexity ML detector is summarized in Algorithm 1.

Algorithm 1 Reduced-Complexity ML Detector for MS-STSK

For every c-th AC in N_c
  For every q-th dispersion matrix in M_Q
    1. Compute $\mathbf{H_c}$
    2. Apply Vectorized MF based on the c-th AC to get $\hat{\mathbf{y}}_{c,q}$
    3. Estimate the transmitted symbol $\hat{s}_l$
      a. QAM?
        Divide into TWO PAM symbols to get (24)
      b. PSK?
        Estimate $\hat{\phi}$ using the angle of $\hat{\mathbf{y}}_{c,q}$
    4. Estimate $< \hat{q},\ \hat{c} >$
  end
end

Nonetheless, the complexity of the detector may be further reduced by choosing an appropriate STSK encoder. Due to the fact that the complexity order of this detector is not affected by the constellation size, in order to encode $B_{STSK} = \log_2(M_c M_Q)$ bits in the STSK codeword, larger constellation sizes and lower number of dispersion matrices can be used. For example, to encode $B_{STSK} = 6$ bits in the STSK encoder, instead of choosing $M_Q = 16$ and $M_c = 4$, we can choose $M_Q = 4$ and $M_c = 16$ in order to further reduce the receiver complexity.

IV. PERFORMANCE RESULTS

In this section we characterize the performance of our proposed MS-STSK system for transmission over Rayleigh channels using the classical Monte-Carlo technique. In our simulations we assume perfect CSI at the receiver side, where $\triangle\theta_c = \pi/7$ and $\triangle\theta_c = \pi/8$ are utilized for our QAM and PSK scheme, respectively. Then, we consider MS-STSK(5,2,2,2,2,8)$|_{\text{PSK}}$,[1] MS-STSK(4,2,2,2,2,4)$|_{\text{QAM}}$ and MS-STSK(5,2,2,2,2,8)$|_{\text{QAM}}$ systems, in conjunction with 8, 4 and 8 TA combinations, respectively, which have an identical throughput.

Figure 11 shows the performance comparison of our MS-STSK systems relying on the optimal ML and HL-ML detectors formulated in (16), (28), respectively. The HL-ML detector is an optimal ML detector, which achieves the same performance as the optimal detector, as shown in Figure 11 for all the MS-STSK systems employed.

Figure 12 shows the effect of using distinct sets of M AEs to convey the implicit AC information, where no common

[1]The notation {$|_{\text{PSK/QAM}}$} denotes the constellation type being employed.

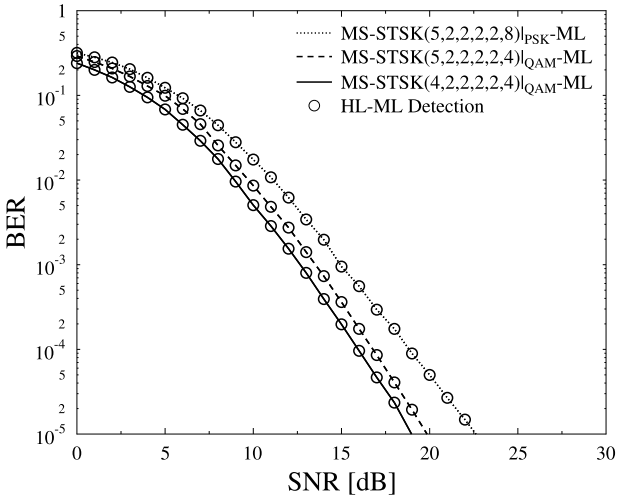

FIGURE 11. BER performance comparison of MS-STSK(5,2,2,2,2,8)$|_{\text{PSK}}$, MS-STSK(5,2,2,2,2,4)$|_{\text{QAM}}$ and MS-STSK(4,2,2,2,2,4)$|_{\text{QAM}}$ systems based on optimal ML and HL-ML detectors.

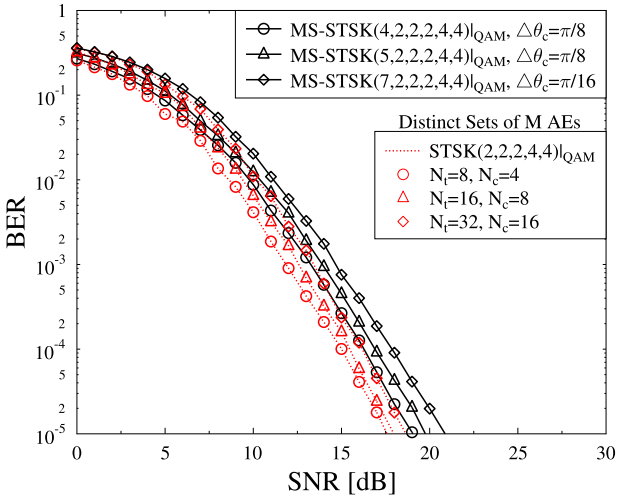

FIGURE 12. The BER performance of three MS-STSK systems using distinct sets of M AEs with STSK(2,2,2,4,4)$|_{\text{QAM}}$ and $N_t = 8$, 16 and 32 AEs compared to their equivalent throughput MS-STSK(4,2,2,2,2,4,4)$|_{\text{QAM}}$, MS-STSK(5,2,2,2,2,4,4)$|_{\text{QAM}}$ and MS-STSK(7,2,2,2,2,4,4)$|_{\text{QAM}}$ systems having $\triangle\theta_c = \pi/8$, $\pi/8$ and $\pi/16$ phase-shifts, respectively.

AEs are allocated to two or more ACs. Consider the set of MS-STSK systems associated with STSK(2,2,2,4,4)$|_{\text{QAM}}$ and $N_t = 8$, 16 and 32 AEs activating distinct sets of $M = 2$ AEs in order to utilize $N_{AC} = 4$, 8 and 16 ACs. This yields a throughput of 7, 8 and 9 bps, respectively, when no phase-shift is applied, i.e. we have $\triangle\theta_c = 0$. These are compared to MS-STSK(4,2,2,2,4,4)$|_{\text{QAM}}$, MS-STSK(5,2,2,2,4,4)$|_{\text{QAM}}$ and MS-STSK(7,2,2,2,4,4)$|_{\text{QAM}}$ associated with the equivalent number of ACs to the above-mentioned systems having the phase-shifts of $\triangle\theta_c = \pi/8$, $\pi/8$ and $\pi/16$, respectively. It is shown in Figure 12 that by employing distinct sets of M AEs, a better performance is achieved in all the three cases due to the higher number of AEs

required to form the required number of ACs, which results in having no antenna correlation between the ACs. However, owing to the fact that not all ACs are actively exploited for data-signalling and each AE is allocated to a single AC, the enhanced performance comes at the cost of reducing the achievable throughput. For instance, given the simulated system STSK(2,2,2,4,4)$|_{\text{QAM}}$ and $N_t = 8$, only $N_c = 4$ ACs are used to transmit $B_{ASU} = 2$ bits, while by fully exploiting the available set of ACs the system is capable of implicitly conveying $\left\lfloor \log_2 \binom{8}{2} \right\rfloor = 4$ bits.

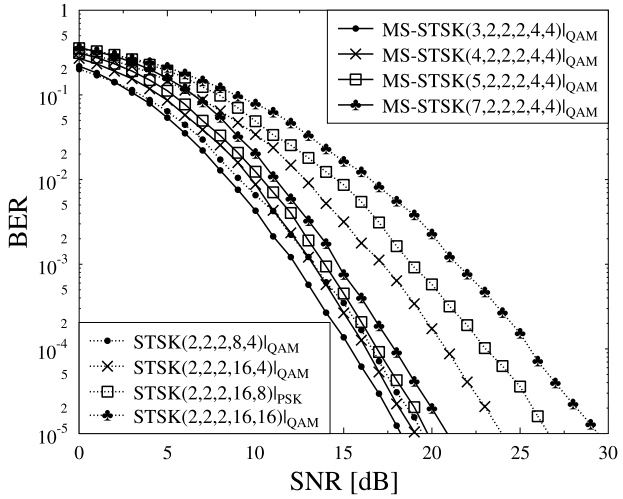

FIGURE 13. The BER performance of MS-STSK(3,2,2,2,4,4)$|_{\text{QAM}}$, MS-STSK(4,2,2,2,4,4)$|_{\text{QAM}}$, MS-STSK(5,2,2,2,4,4)$|_{\text{QAM}}$ and MS-STSK(7,2,2,2,4,4)$|_{\text{QAM}}$ systems having 2, 4, 8 and 16 ACs associated with the phase-shifts of $\Delta\theta_c = \pi, \pi/8, \pi/8$ and $\pi/16$ and symbol rates of 5, 6, 7 and 8 BPC, respectively, compared to their STSK equivalent systems STSK(2,2,2,8,4)$|_{\text{QAM}}$, STSK(2,2,2,16,4)$|_{\text{QAM}}$, STSK(2,2,2,16,8)$|_{\text{PSK}}$ and STSK(2,2,2,16,16)$|_{\text{QAM}}$, respectively.

Figure 13 illustrates the BER performances of different MS-STSK systems compared to their equivalent-throughput STSK counterparts. Consider the MS-STSK (3,2,2,2,4,4)$|_{\text{QAM}}$, MS-STSK(4,2,2,2,4,4)$|_{\text{QAM}}$, MS-STSK(5,2,2,2,4,4)$|_{\text{QAM}}$ and MS-STSK(7,2,2,2,4,4)$|_{\text{QAM}}$ systems having 2, 4, 8 and 16 ACs associated with the phase-shifts of $\Delta\theta_c = \pi, \pi/8, \pi/8$ and $\pi/16$ and symbol rates of 5, 6, 7 and 8 BPC, respectively. Moreover, to compare the MS-STSK performance to that of the existing STSK, we consider the STSK(2,2,2,8,4)$|_{\text{QAM}}$, STSK(2,2,2,16,4)$|_{\text{QAM}}$, STSK(2,2,2,16,8)$|_{\text{PSK}}$ and STSK(2,2,2,16,16)$|_{\text{QAM}}$ system having the same MS-STSK symbol rates. The MS-STSK scheme achieves a gradually improving BER advantage, as the throughput increases, where the smallest difference is observed between the systems associated with the lowest symbol rate, namely for the MS-STSK(3,2,2,2,4,4)$|_{\text{QAM}}$ and STSK(2,2,2,8,4)$|_{\text{QAM}}$. On the other hand, MS-STSK(4,2,2,2,4,4)$|_{\text{QAM}}$, MS-STSK(5,2,2,2,4,4)$|_{\text{QAM}}$ and MS-STSK(7,2,2,2,4,4)$|_{\text{QAM}}$ have beneficial performance gains of about 4, 6.5 and 8 dB over their STSK counterparts. Hence, as the number of bits conveyed increases, the MS-STSK scheme has a gradually improving BER advantage over its STSK benchmark.

Furthermore, the results of Figure 13 reveal that at the same throughput, an MS-STSK system may obtain a better BER performance at the same complexity order as its STSK counterpart. For instance, both the MS-STSK(3,2,2,2,4,4)$|_{\text{QAM}}$ and STSK(2,2,2,8,4)$|_{\text{QAM}}$ systems are capable of maintaining the same complexity order of $\mathcal{O}(32)$ and $\mathcal{O}(8)$, when using ML based and HL-ML based detectors, respectively, but the MS-STSK scheme has an enhanced system performance. However, by comparing the performance of MS-STSK(5,2,2,2,4,4)$|_{\text{QAM}}$ and STSK(2,2,2,16,8)$|_{\text{PSK}}$, the complexity order of MS-STSK system using a HL-ML detector is $\mathcal{O}(N_c M_Q) = \mathcal{O}(8 \times 4) = \mathcal{O}(32)$, which is higher than that of the STSK system associated with an equivalent detector of a complexity order of $\mathcal{O}(M_Q) = \mathcal{O}(16)$. The complexity order of the MS-STSK scheme can be further reduced by using $M_Q = 2$ and $M_c = 8$ rather than using $M_Q = 4$ and $M_c = 4$, where both achieve the same throughput. A comparison between all the simulated MS-STSK and STSK systems of Figure 13 is explicitly summarized in Table 2. Furthermore, the table shows the number of ACs, the complexity orders of the ML and HL-ML detectors and the SNR required at BER=10^{-5} by the MS-STSK and STSK systems characterized in Figure 13. The increased complexity orders of the MS-STSK systems over their STSK counterparts when employing the HL-ML detector do not specifically imply that the MS-STSK system imposes a higher complexity order. However, depending on the system configurations specified in terms of M_c, M_Q and N_c, both systems impose the same complexity orders.

TABLE 2. Comparison between the MS-STSK and STSK schemes having ML and HL-ML detectors in terms of complexity order and SNR required at BER = 10^{-5}.

Throughput (BPS)		**5**	**6**	**7**	**8**
$\binom{N_t}{N_{RF}}$		$\binom{3}{2}$	$\binom{4}{2}$	$\binom{5}{2}$	$\binom{7}{2}$
N_{AC}		2	4	8	16
MS-STSK	Complexity Order (ML)	$\mathcal{O}(32)$	$\mathcal{O}(64)$	$\mathcal{O}(128)$	$\mathcal{O}(256)$
	Complexity Order (HL-ML)	$\mathcal{O}(8)$	$\mathcal{O}(16)$	$\mathcal{O}(32)$	$\mathcal{O}(64)$
	$SNR_{BER=10^{-5}}$ [dB]	18	19.1	19.5	21
STSK	Complexity Order (ML)	$\mathcal{O}(32)$	$\mathcal{O}(64)$	$\mathcal{O}(128)$	$\mathcal{O}(256)$
	Complexity Order (HL-ML)	$\mathcal{O}(8)$	$\mathcal{O}(16)$	$\mathcal{O}(16)$	$\mathcal{O}(16)$
	$SNR_{BER=10^{-5}}$ [dB]	19	23.5	26	29

V. CONCLUSIONS

This paper presented a novel MIMO system referred to as MS-STSK, which is capable of striking a flexible multiplexing vs diversity gain. In addition to the STSK codeword, additional implicit information is conveyed through the AC indices, where the total number of TAs is higher than the available RF chains. This technique supports higher data rates than the standard multifunctional STSK scheme at low number of RF chains. Furthermore, employing STSK encoding adds more reliability to the system, where the diversity order and STSK throughput can be flexibly tuned according to the design requirements. We also conceived a low-complexity optimal detector in order to reduce the overall detection complexity from $\mathcal{O}(M_Q M_c N_c)$ to $\mathcal{O}(M_Q N_c)$, while maintaining the optimal system performance.

REFERENCES

[1] L. Hanzo, H. Haas, S. Imre, D. O'Brien, M. Rupp, and L. Gyongyosi, "Wireless myths, realities, and futures: From 3G/4G to optical and quantum wireless," *Proc. IEEE*, vol. 100, pp. 1853–1888, May 2012.

[2] A. Bleicher. (Jun. 2013). *Telecom Wireless News Millimeter Waves May be the Future of 5G Phones*. [Online]. Available: http://spectrum.ieee.org/telecom/wireless/millimeter-waves-may-be-the-future-of-5g-phones

[3] T. S. Rappaport *et al.*, "Millimeter wave mobile communications for 5G cellular: It will work!" *IEEE Access*, vol. 1, pp. 335–349, May 2013.

[4] J. Ling, D. Chizhik, C. S. Chen, and R. A. Valenzuela, "Capacity growth of heterogeneous cellular networks," *Bell Labs Tech. J.*, vol. 18, no. 1, pp. 27–40, Jun. 2013.

[5] L. Hanzo, M. El-Hajjar, and O. Alamri, "Near-capacity wireless transceivers and cooperative communications in the MIMO era: Evolution of standards, waveform design, and future perspectives," *Proc. IEEE*, vol. 99, no. 8, pp. 1343–1385, Aug. 2011.

[6] L. Hanzo, O. Alamri, M. El-Haijar, and N. Wu, *Advanced Space-Time Coding: Near-Capacity Sphere-Packing, Multi-Functional MIMOs and Cooperative Space-Time Processing*. New York, NY, USA: Wiley, 2008. [Online]. Available: http://eprints.soton.ac.uk/265783/

[7] P. W. Wolniansky, G. J. Foschini, G. D. Golden, and R. A. Valenzuela, "V-BLAST: An architecture for realizing very high data rates over the rich-scattering wireless channel," in *Proc. Int. Symp. Signals, Syst., Electron. (ISSSE)*, Sep./Oct. 1998, pp. 295–300.

[8] S. Alamouti, "A simple transmit diversity technique for wireless communications," *IEEE J. Sel. Areas Commun.*, vol. 16, no. 8, pp. 1451–1458, Oct. 1998.

[9] V. Tarokh, H. Jafarkhani, and A. R. Calderbank, "Space-time block codes from orthogonal designs," *IEEE Trans. Inf. Theory*, vol. 45, no. 5, pp. 1456–1467, Jul. 1999.

[10] M. El-Hajjar, O. Alamri, J. Wang, S. Zummo, and L. Hanzo, "Layered steered space-time codes using multi-dimensional sphere packing modulation," *IEEE Trans. Wireless Commun.*, vol. 8, no. 7, pp. 3335–3340, Jul. 2009.

[11] R. Y. Mesleh, H. Haas, S. Sinanovic, C. W. Ahn, and S. Yun, "Spatial modulation," *IEEE Trans. Veh. Technol.*, vol. 57, no. 4, pp. 2228–2241, Jul. 2008.

[12] M. Di Renzo, H. Haas, A. Ghrayeb, S. Sugiura, and L. Hanzo, "Spatial modulation for generalized MIMO: Challenges, opportunities, and implementation," *Proc. IEEE*, vol. 102, no. 1, pp. 56–103, Jan. 2014.

[13] P. Yang, M. D. Renzo, Y. Xiao, S. Li, and L. Hanzo, "Design guidelines for spatial modulation," *IEEE Commun. Surveys Tuts.*, vol. 17, no. 1, pp. 6–26, 1st Quart., 2015.

[14] P. Yang *et al.*, "Single-carrier spatial modulation: A promising design for large-scale broadband antenna systems," *IEEE Commun. Surveys Tuts.*, vol. PP, no. 99, pp. 11.

[15] B. Hassibi and B. Hochwald, "Linear dispersion codes," in *Proc. IEEE Int. Symp. Inf. Theory*, Jun. 2001, p. 325.

[16] R. W. Heath, Jr., and A. Paulraj, "Linear dispersion codes for MIMO systems based on frame theory," *IEEE Trans. Signal Process.*, vol. 50, no. 10, pp. 2429–2441, Oct. 2002.

[17] S. Sugiura, S. Chen, and L. Hanzo, "Generalized space-time shift keying designed for flexible diversity-, multiplexing- and complexity-tradeoffs," *IEEE Trans. Wireless Commun.*, vol. 10, no. 4, pp. 1144–1153, Apr. 2011.

[18] J. Wang, S. Jia, and J. Song, "Generalised spatial modulation system with multiple active transmit antennas and low complexity detection scheme," *IEEE Trans. Wireless Commun.*, vol. 11, no. 4, pp. 1605–1615, Apr. 2012.

[19] S. Sugiura, C. Xu, S. XinNg, and L. Hanzo, "Reduced-complexity iterative-detection-aided generalized space-time shift keying," *IEEE Trans. Veh. Technol.*, vol. 61, no. 8, pp. 3656–3664, Oct. 2012.

[20] M. C. Lee, W. H. Chung, and T. S. Lee, "Generalized precoder design formulation and iterative algorithm for spatial modulation in MIMO systems with CSIT," *IEEE Trans. Commun.*, vol. 63, no. 4, pp. 1230–1244, Apr. 2015.

[21] E. Basar, U. Aygolu, E. Panayirci, and H. V. Poor, "Space-time block coded spatial modulation," *IEEE Trans. Commun.*, vol. 59, no. 3, pp. 823–832, Mar. 2011.

[22] T. Datta, H. Eshwaraiah, and A. Chockalingam, "Generalized space and frequency index modulation," *IEEE Trans. Veh. Technol.*, vol. PP, no. 99, pp. 11.

[23] S. Sugiura, C. Xu, S. X. Ng, and L. Hanzo, "Reduced-complexity coherent versus non-coherent QAM-aided space-time shift keying," *IEEE Trans. Commun.*, vol. 59, no. 11, pp. 3090–3101, Nov. 2011.

[24] C. Xu, S. Sugiura, S. X. Ng, and L. Hanzo, "Spatial modulation and space-time shift keying: Optimal performance at a reduced detection complexity," *IEEE Trans. Commun.*, vol. 61, no. 1, pp. 206–216, Jan. 2013.

[25] R. Rajashekar, K. V. S. Hari, and L. Hanzo, "Reduced-complexity ML detection and capacity-optimized training for spatial modulation systems," *IEEE Trans. Commun.*, vol. 62, no. 1, pp. 112–125, Jan. 2014.

[26] A. J. Paulraj and B. C. Ng, "Space-time modems for wireless personal communications," *IEEE Pers. Commun.*, vol. 5, no. 1, pp. 36–48, Feb. 1998.

[27] S. Kay, *Fundamentals of Statistical Signal Processing: Estimation Theory* (Prentice Hall Signal Processing Series), vol. 1. Upper Saddle River, NJ, USA: Prentice-Hall, 2013. [Online]. Available: http://opac.inria.fr/record=b1082640

[28] S. Chen, A. Livingstone, and L. Hanzo, "Minimum bit-error rate design for space-time equalization-based multiuser detection," *IEEE Trans. Commun.*, vol. 54, no. 5, pp. 824–832, May 2006.

[29] Y. Yang and B. Jiao, "Information-guided channel-hopping for high data rate wireless communication," *IEEE Commun. Lett.*, vol. 12, no. 4, pp. 225–227, Apr. 2008.

[30] M. Kadir, S. Sugiura, S. Chen, and L. Hanzo, "Unified MIMO–multicarrier designs: A spaceŰtime shift keying approach," *IEEE Commun. Surveys Tuts.*, vol. 17, no. 2, pp. 550–579, 2nd Quart., 2015.

[31] I. A. Hemadeh, M. El-Hajjar, S. Won, and L. Hanzo, "Layered multi-group steered space-time shift-keying for millimeter-wave communications," *IEEE Access*, vol. PP, no. 99, pp. 11.

[32] H. Men and M. Jin, "A low-complexity ML detection algorithm for spatial modulation systems with *M* PSK constellation," *IEEE Commun. Lett.*, vol. 18, no. 8, pp. 1375–1378, Aug. 2014.

[33] C. Masouros and L. Hanzo, "Constellation-randomization achieves transmit diversity for single-RF spatial modulation," *IEEE Trans. Veh. Technol.*, vol. 18, no. 8, pp. 1375–1378, Aug. 2014.

IBRAHIM A. HEMADEH received the B.Eng. degree (Hons.) in computer and communications engineering from the Islamic University of Lebanon in 2010 and the M.Sc. degree (Hons.) in wireless communications from the University of Southampton, U.K., in 2012. He is currently pursuing the Ph.D. degree in wireless communications with the Univesrity of Southampton under the supervision of Prof. L. Hanzo and Dr. M. El-Hajjar. His research interests mainly include millimeter-wave communications, multi-functional MIMO and multi-user MIMO.

MOHAMMED EL-HAJJAR received the B.Eng. degree in electrical engineering from the American University of Beirut, Lebanon, in 2004, and the M.Sc. degree in radio frequency communication systems and the Ph.D. degree in wireless communications from the University of Southampton, U.K., in 2005 and 2008, respectively. Following the Ph.D. degree, he joined Imagination Technologies as a Design Engineer, where he worked on designing and developing Imagination's multi-standard communications platform, which resulted in three patents. In 2012, he joined the Electronics and Computer Science with the University of Southampton as a Lecturer with the Southampton Wireless Research Group. He is currently a Lecturer in electronics and computer science with the University of Southampton. He is the recipient of several academic awards, including the Dean's Award for creative achievement, the Dorothy Hodgkin Postgraduate Award, and the IEEE ICC 2010 Best Paper Award. He has published a Wiley-IEEE book and in excess of 60 journal and international conference papers. His research interests are mainly in the development of intelligent communications systems, including energy-efficient transceiver design, MIMO, millimeter-wave communications, and radio over fiber systems.

SEUNGHWAN WON (M'04) received the B.S. and M.S. degrees in radio science and engineering from Korea University, Seoul, South Korea, in 1999 and 2001, respectively, and the Ph.D. degree from the Communications Research Group, School of Electronics and Computer Science, University of Southampton, U.K., in 2008. He was a Research Engineer with the Mobile Communication Technology Research Laboratory, LG Electronics R&D, from 2001 to 2004. In 2013, he was appointed as an Associate Professor by the University of Southampton. Upon completing the Ph.D. degree, he returned to his native South Korea and joined Samsung, where he is currently teaching and conducting research with the University of Southampton, Johor, Malaysia. He published a host of papers in these research fields. His major research interests included initial synchronization in noncoherent MIMO aided single- and multi-carrier CDMA, IDMA, and OFDMA, and in iterative synchronization schemes designed for MIMO aided single- and multi-carrier transmission systems. He was a recipient of the 2004 State Scholarship of the Information and Telecommunication National Scholarship Program, Ministry of Information and Communication, South Korea.

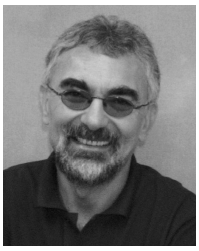

LAJOS HANZO received the degree in electronics in 1976 and the Ph.D. degree in 1983. In 2009, he was awarded the Honorary Doctorate Doctor Honoris Causa by the Technical University of Budapest. During his 38-year career in telecommunications, he has held various research and academic positions in Hungary, Germany, and the U.K. Since 1986, he has been with the School of Electronics and Computer Science, University of Southampton, U.K., where he holds the Chair in telecommunications. He has successfully supervised about 100 Ph.D. students, co-authored 20 John Wiley/IEEE Press books on mobile radio communications totaling in excess of 10 000 pages, published over 1500 research entries at the IEEE Xplore, acted both as TPC and General Chair of the IEEE conferences, presented keynote lectures, and has been awarded a number of distinctions. He is currently directing 100 strong academic research teams, working on a range of research projects in the field of wireless multimedia communications sponsored by industry, the Engineering and Physical Sciences Research Council U.K., the European Research Council's Advanced Fellow Grant, and the Royal Society's Wolfson Research Merit Award. He is an enthusiastic supporter of industrial and academic liaison and he offers a range of industrial courses.